Through Thick and Thin: Imaging Through Obscurant using SPAD array

Joyce Mau*, Vladimyros Devrelis†, Geoffrey Day*, Graeme Nash*, Jochen Trumpf‡ and Dennis Delic*
*Defence Science Technology Group
Edinburgh, Australia
Email: ManChing.Mau@dst.defence.gov.au
†Ballistic Systems Pty Ltd, Edinburgh, Australia
‡Software Innovation Institute
Australian National University, Canberra, Australia
Email: jochen.trumpf@anu.edu.au

***Abstract*—Preliminary work on 3D image collection and classification of targets in the presence of obscurant using a Flash LiDAR system is discussed in this paper. The system is based around a DST designed 32 x 32 Single Photon Avalanche Diode (SPAD) array to image either targets or silhouettes of targets. The collected data included military targets that were obscured either by camouflage nets or fog. For camouflage net, the target was detected using an algorithm implemented on the Nvidia Jetson TX2. Targets obscured by fog are detected and classified where the classification accuracy is 100% for fog visibility down to 17.3m and 89.5% for 14.1m. This algorithm was not implemented on the TX2 but its simplicity shows potential for it in the future. This initial approach opens the road to eventually operate SPAD based systems for real-time classification through dust or smoke.**

I. Introduction

Rapid advances in modern cameras (visible, hyperspectral and thermal) have seen increasing pixel resolutions, lower size, weight and power usage. These properties make them favourable for remote surveillance applications, easily supported by small Unmanned Aerial Systems (UAS) for autonomous detection and classification of targets. However, a disadvantage of passive imaging cameras despite their high pixel resolutions is their poor performance when trying to distinguish targets hidden by natural or man-made obscurant such as fog or camouflage nets. An active imaging system such as a Single Photon LiDAR (SPL) using a Single Photon Avalanche Diode (SPAD) array sensor can provide a solution. Advanced SPL systems offer the Defence war fighter a tactical advantage in the battlefield, providing improved rapid environment assessment, sensing and data collection capabilities.

A SPAD is a highly sensitive photodiode with the ability to detect a single photon. This allows it to see in low light conditions, and when combined with a pulsing laser, can perform photon timing to measure a photon's Time-of-Fight (ToF) - information which can be used to generate a 3D image. The high sensitivity of the SPAD sensor allows it to register the faintest return from the target even when hidden behind obscurant. Employing range/time-gating techniques on the returning photons it is then possible to remove a high degree of background noise and clutter. With the application of simple image post processing techniques, the signal-to-noise ratio (SNR) can be improved further allowing the detector to extract the target shape from the scene with clarity.

In this paper, we present the detection of targets in the presence of obscurant using a DST developed 3D Flash SPL system involving a first generation designed DST 32 x 32 SPAD array camera. The signal strength of photon returns detected by the SPAD camera are dependent on both the noise characteristics of the sensor and environmental background noise. Previous work involved using a single SPAD sensor as a ToF scanner of the obscured scene and a 1550nm pulsing laser to image through camouflage nets, fog and smoke in various outdoor and indoor locations [1], [2]. While other previous work involved using a different 32x32 SPAD array camera and a 580nm pulsing laser to image through fog but in a small 0.5x0.5x1 m^3 chamber [3], [4]. This work evaluates the utility of SPAD sensors in imaging obscured targets at greater ranges using a Flash LiDAR technique, with a SPAD array sensor tuned to a 532nm laser illuminator.

Both outdoor and indoor imaging activities were conducted for this demonstration. An outdoor trial was executed to image the target behind the camouflage net. Another trial was conducted indoors to image targets through fog. Detection is applied to extract the targets, and classification is applied to distinguish the targets in fog. The detection algorithm is demonstrated on the Nvidia Jetson TX2.

II. Image Collection

The LiDAR system used for image collection in this paper is shown in Fig. 1a. The SPAD microchip was designed as a planar device in a standard CMOS 130nm process. Its active area is 20 μm in diameter and uses a passive quenching front-end circuit which is on the same die. Micro-lensing was used to improve its fill-factor. Optically, a narrow 2nm band filter centred at 532nm (Edmund Optics part no. 68-970) and the Pentax TV Zoom lens 12.5 to 75 mm with F number of 1 to 1.8 were used. The bias voltage is at 29.1V, with the dark count rate being 2000-6000 cps. The digital and analogue circuitry operated on $1.8V$ and $3.3V$. The coupled laser had a wavelength of 532 nm, a pulse energy of 35 mJ and a pulse

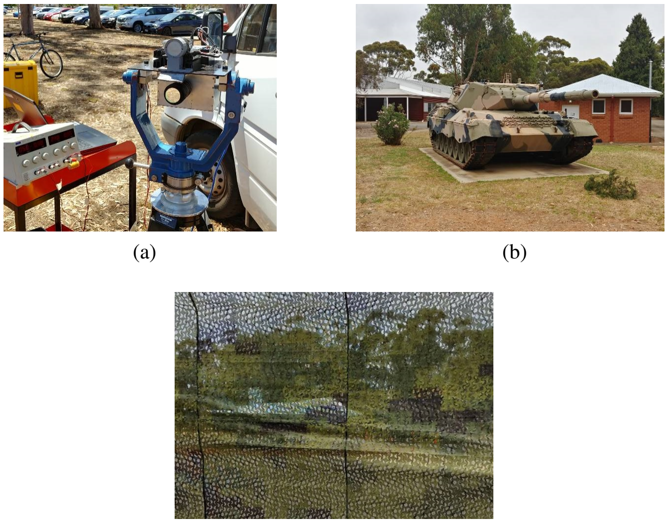

(a) (b) (c)

Fig. 1. (a) DST built SPAD based LiDAR system in field. (b) Leopard AS1 main battle tank. (c) The Ironbird model aircraft behind camouflage net.

length of 5 ns which resulted in a range resolution of 0.75 m and a pulse repetition frequency of 20 Hz. 532nm was chosen because it was easy to obtain lasers in this wavelength with high powers and it is close to the SPAD's peak photon detection efficiency of 11%. A diffuser was placed in front of the laser to make it eye safe and this resulted in a laser beam divergence of approximately 115 degrees. These parameters remained the same for all image collections. The values in the collected images are in terms of clock cycles which is equivalent to distances by multiplying them with the range resolution value.

A. Overview of the outdoor trials

Field trials were conducted over several days at the DST Edinburgh site with the intent to image a Leopard AS1 main battle tank (as shown in Figure 1b) and a DST Ironbird F-35 research model aircraft (see Figure 1c) through camouflage netting. The LiDAR system was mounted on a tripod 1.5 m above ground level. On the ground, the targets were placed 30 m to 50 m from the LiDAR.

The LiDAR field of view was adjusted so that the objects being imaged filled the 32x32 pixels. The LiDAR system was used to measure the ToF of the first photon received by each pixel in the SPAD array. Imaging data were collected in daylight during morning and afternoon but noon was avoided in order to reduce noise due to excess of solar photons which reduced the signal-to-noise ratio (SNR) to less than 1.5. Similar treatment of improving the signal from the Poisson and solar noise is discussed in [5] and [6]. A camouflage net was erected in front of the targets with the intention to obscure the field of view. The net is a Saab multispectral net called the Ultra-Lightweight Camouflage Screen (ULCAS).

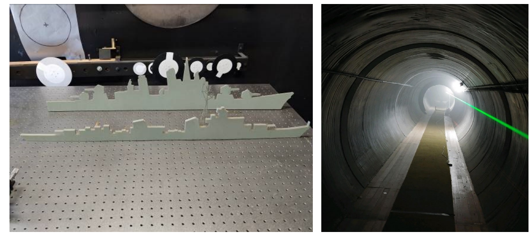

(a) (b)

Fig. 2. (a) Cutout sillouetes of ships. (b) shows the tunnel with lights on with the testing target barely visible. Experiments are conducted in the dark. The visibility here is 13.8m which is calculated from laser attenuation measurements of the thin continuous laser beam on the right.

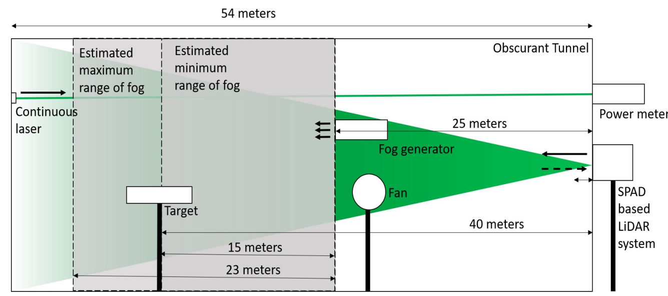

Fig. 3. Setup of tunnel for measurements through fog.

B. Overview of the indoor lab trial

Experimental work was conducted in a dedicated 54m long dark tunnel laboratory to image ship silhouettes through fog. Figure 2a shows the two silhouettes used but in the experiments they were painted white. One is representative of a Skoryy Class (USSR) destroyer and is 120.5m long, and the other is a mock DDG destroyer and is 133m long. The original Skoryy class were the first destroyers built for the Soviet Navy after World War II. The DDG were Perth-class destroyers operated by the Royal Australian Navy. The fog generator called the Rave AF1214 Fog Machine was used to obscure the targets and was placed at 25m away from the LiDAR system. The fog liquid used is the Rave heavy fog water-based liquid. Figure 3 shows a schematic of the setup. The fog is assumed to start at that point because a fan is used to keep the fog from moving towards the LiDAR system at the start of the tunnel and enable even mixing. This can be seen in Figure 2b where the start of the tunnel does not have fog. The fog is found to end between 15m and 23m from the generator, and the target is placed at 15 m from the generator. The LiDAR system was range gated to measure the time of flight of the first photon received by each pixel in the SPAD array from that range gate. Imaging data were collected in the dark which reduced environmental noise thus improving the SNR as compared to the outdoor trial.

The average visibility of the fog in that area varies between 76.9m to 14.1m. This measurement describes how far can the naked eye see from the fog generator. These values are calculated from measuring the transmittance of a continuous

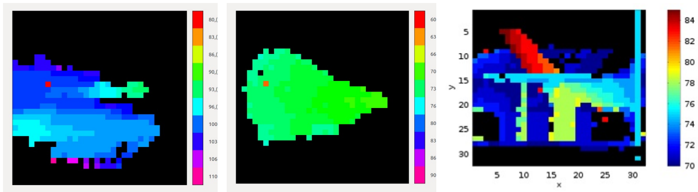

(a) (b) (c)

Fig. 4. (a) LiDAR Image of the tank. (b) Extracted LiDAR Image of the aircraft bow and cockpit behind camouflage net. (c) Extracted LiDAR Image of the aircraft wing and empennage behind camouflage net.

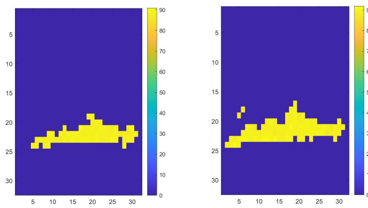

(a) (b)

Fig. 5. Extracted LiDAR Image of ship at 14.1m from the start of the fog where (a) is a Skoryy Class (USSR) destroyer, and (b) is a mock DDG destroyer. Note: the start of the fog is 25m away from the system.

532 nm laser beam over 19m, which is the average length at which the fog ends from the generator. The average length is used since it is difficult to measure the exact distribution of fog for each imaging condition and the equations assume uniform distribution of fog. The attenuation coefficient of the laser is calculated using Beer-Lambert's Law [7] and then the coefficient value to used to calculate the visibility value [8]. It is assumed that there is negligible laser power dissipation in the area without fog.

III. Detection of target behind camouflage net

Denoising of the collected data sets is achieved via histogram averaging of anything between 50 to 500 frames. A histogram is formed for each pixel and then the corrected distance is selected as the range of the maximum of the histogram. The logic behind this is that photons from the laser that have hit the target will be at the same range in each frame while photons from other sources (such as the sun or due to shot noise) will have random range values with a uniform distribution. A threshold is applied to the histogram such that no detection is registered for pixels that have a histogram with no clear peak. This method is used to extract the targets imaged behind a camouflage net described in Section II-A. The extracted Leopard AS1 main battle tank is shown in Figure 4a and parts of the research model aircraft are shown in Figures 4b and 4c. All these images are only parts of the target since the SPAD camera's field of view cannot fit the whole target. This is due to its low resolution. In practice, multiple images can be stitched together for the entire target's image. In addition, the detection algorithm is implemented onto a single board computer of type Nvidia Jetson TX2 to demonstrate that it can be executed on-board a portable system.

IV. Detection and Classification of target obscured by fog

A series of processing steps is applied to distinguish a frigate from the noisy environment in the image. First of all, the histogram algorithm as described in Section III is used. Further processing is then applied by comparing each pixel's value with its surrounding pixels. The pixel is discarded if it is within 3 clock cycles of less than four of its surrounding 3x3 pixels. This is to remove the noisy background where the pixel values are random. For the maximum fog condition where visibility reduces to 14.1m, only pixels with less than 2 correlated pixels are discarded. At this stage, it can be determined that there is a distinction in the number of clock cycles between the target and the background. Therefore, a threshold value is used to further filter out the noise which should result in a clear image as shown in Figure 5, where images of both frigates are shown.

For classification, the target's area is the sole metric used because the margin between the area values of the two frigates at different fog conditions is large enough for classification. The total number of non-zero pixels in the processed image are summed to calculate the area. An average area for each target is calculated from 100 processed frames and then a different set of 100 processed frames are used for testing. The classification algorithm is based on which frigate's mean area is closer to the testing target's area value. The average accuracy result is 100% for all visibility conditions down to 17.3m. The average accuracy for the visibility condition of 14.1m is 89.5%, which is the location of the target. The accuracy decreases because the margin between the two groups of area values reduces to under 10 clock cycles. Furthermore, these detection and classification results demonstrate the superior capability of SPAD LiDAR system because given a scenario where the visibility is low and the scene looks similar to Figure 2b, it is difficult to detect and classify the target with the naked eye. However, the SPAD LiDAR can do so where Figure 5 shows the clear imagery after processing.

V. Conclusion

This paper discussed the work on 3D imaging and classification of military targets using a Flash SPL system. The experimentally collected target data was then extracted from the Flash LiDAR images and a classification technique was applied. The classification accuracy of 89.5% at a 14.1m visibility was demonstrated using a simple classifier based on area. This study highlights the detection and classification performance of a SPAD array sensor with a low spatial resolution and shows that this system has the potential for real time classification of defence targets from UASs.

Acknowledgement

The authors wish to thank Mr Carey Schiller, for his support and assistance in some of the field trials.

REFERENCES

[1] R. Tobin, A. Halimi, A. McCarthy, M. Laurenzis, F. Christnacher, and G. S. Buller, “Three-dimensional single-photon imaging through obscurants,” *Opt. Express*, vol. 27, no. 4, p. 4590, Feb. 2019. [Online]. Available: https://www.osapublishing.org/abstract.cfm?URI=oe-27-4-4590

[2] R. Tobin *et al.*, “Long-range depth profiling of camouflaged targets using single-photon detection,” *Opt. Eng.*, vol. 57, no. 03, p. 031303, Dec. 2017. [Online]. Available: https://www.spiedigitallibrary.org/journals/optical-engineering/volume-57/issue-03/031303/Long-range-depth-profiling-of-camouflaged-targets-using-single-photon/10.1117/1.OE.57.3.031303.full

[3] G. Satat, M. Tancik, O. Gupta, B. Heshmat, and R. Raskar, “Object classification through scattering media with deep learning on time resolved measurement,” *Opt. Express*, vol. 25, no. 15, p. 17466, Jul. 2017. [Online]. Available: https://www.osapublishing.org/abstract.cfm?URI=oe-25-15-17466

[4] G. Satat, M. Tancik, and R. Raskar, “Towards photography through realistic fog,” in *2018 IEEE Int. Conf. on Comput. Photography (ICCP)*, Pittsburgh, PA, May 2018, pp. 1–10. [Online]. Available: https://ieeexplore.ieee.org/document/8368463/

[5] A. D. Ruvalcaba-Cardenas, T. Scoleri, and G. Day, “Object Classification using Deep Learning on Extremely Low-Resolution Time-of-Flight Data,” in *2018 Digit. Image Comput.: Techn. and Appl. (DICTA)*, Canberra, Australia, Dec. 2018, pp. 1–7. [Online]. Available: https://ieeexplore.ieee.org/document/8615877/

[6] J. Mau *et al.*, “Embedded implementation of a random feature detecting network for real-time classification of time-of-flight SPAD array recordings,” in *Laser Radar Technology and Applications XXIV*, Baltimore, United States, May 2019, p. 7. [Online]. Available: https://www.spiedigitallibrary.org/conference-proceedings-of-spie/11005/2517875/Embedded-implementation-of-a-random-feature-detecting-network-for-real/10.1117/12.2517875.full

[7] F. G. Smith, J. S. Accetta, and D. L. Shumaker, “Transmission along a Slant Path,” in *The Infrared & Electro-Optical Systems Handbook - Atmospheric Propagation of Radiation*. Michigan: ERIM and Infrared Information Analysis Center, 1993, vol. 2, pp. 112–115.

[8] ——, “Visibility Range,” in *The Infrared & Electro-Optical Systems Handbook - Atmospheric Propagation of Radiation*. Michigan: ERIM and Infrared Information Analysis Center, 1993, vol. 2, pp. 123–127.